JOURNAL OF APPLIED ELECTROCHEMISTRY **24** (1994) 227–232

Effects of saccharin and aliphatic alcohols on the electrocrystallization of nickel

Y. NAKAMURA,

Research Institute, Orion Machinery Co., Ltd, 521-1 Wakasato, Nagano 380, Japan

N. KANEKO, M. WATANABE, H. NEZU

Faculty of Engineering, Shinshu University, 500 Wakasato, Nagano 380, Japan

Received 13 May 1993; revised 18 July 1993

The effects of saccharin and three kinds of aliphatic alcohols (*n*-propyl alcohol, allyl alcohol, propargyl alcohol) on the surface morphology and crystal orientation of electrodeposited nickel from a Watts bath (1 M $NiSO_4$ + 0.2 M $NiCl_2$ + 0.5 M H_3BO_3) have been studied by means of electrochemical methods, scanning electron microscopy, energy-dispersive X-ray analysis and measurements of X-ray diffraction patterns. Saccharin and three kinds of aliphatic alcohols were adsorbed on the electrode and inhibited the reduction of nickel ion. The inhibitory effect on the reduction of nickel ion increased in the order *n*-propyl alcohol, allyl alcohol and propargyl alcohol. Large granular electrodeposits were obtained from the Watts bath in the absence of organic additives. When saccharin was added, fine-grained crystals were observed and the surface roughness was relatively small. When aliphatic alcohols were added, the size of surface morphological features became smaller in the order *n*-propyl alcohol, allyl alcohol and propargyl alcohol. Fine-grained, compact and smooth nickel electrodeposits, which had a preferred orientation with a (1 1 1) plane parallel to the surface, were obtained from the Watts bath containing both saccharin and propargyl alcohol.

1. Introduction

To obtain bright and commercially acceptable nickel deposits it has been found that a combination of several organic additives must be added to Watts baths. Brighteners are classified into first class (characterized by the group $=C-SO_2$ in the molecule) and second class (characterized by the presence of an unsaturated group C=O, C=C, C≡C, C=N and C≡N in the molecule); these two types of brighteners are used together [1, 2]. Further, a number of authors have published papers on the structure and surface morphology of nickel electrodeposits from Watts baths containing organic additives [3–6]. However, the electrochemical characteristics (i.e. adsorption on the electrode, inhibitory effects on the reduction of nickel ion, etc.) of such organic additives have not been systematically studied.

The present authors have already reported the electrochemical behaviour of saccharin and three kinds of diol compounds (butanediol, butenediol, butynediol), and the inhibitory effects of such organic additives on the electrocrystallization of nickel from the Watts bath [7]. As a result, it became apparent that smooth and compact electrodeposits of nickel were obtained by adding both saccharin and butynediol. The purpose of this investigation was to study the electrochemical characteristics of three kinds of aliphatic alcohols (*n*-propyl alcohol, allyl alcohol, propargyl alcohol) and the effects of both saccharin and aliphatic alcohols on the surface morphology and the crystal orientation of electrodeposited nickel from Watts baths.

2. Experimental details

2.1. *Apparatus and procedure*

Electrocapillary curves were obtained by plotting the drop time of mercury against the applied potential using a Yanagimoto Model P-1100 polarograph. The dropping mercury electrode had the following characteristics; a mercury height of 60 cm; mercury flow rate, $m = 1.71\,\mathrm{mg\,s^{-1}}$; drop time, $t = 4.31$ s (in 1 M potassium chloride solution, open circuit). Potentiostatic electrolyses and galvanostatic electrolyses were carried out using a Hokuto Denko Model HA-310 potentiostat–galvanostat. Current–potential curves under potentiostatic conditions were obtained by plotting the steady state current after 30 s from the beginning of electrolysis against the applied potential. The surface morphology of electrodeposited nickel was observed using a Nihon Denshi Model JSM-5400 scanning electron microscope. The X-ray elemental composition map of electrodeposited nickel was observed with a Nihon Denshi Model JED-2001 energy-dispersive X-ray microanalyser combined with the scanning electron microscope. X-ray diffraction patterns of the electrodeposited nickel were obtained using a Rigaku Denki Model

RAD-IA X-ray diffractometer with CuK_α radiation of 0.154 nm wavelength.

The composition of the Watts bath was 1 M nickel sulphate, 0.2 M nickel chloride and 0.5 M boric acid. In this solution, boric acid acts as a buffer to maintain the pH at 4.5–5.5 and chloride ion acts as a nickel-anode corrodant. In the case where the dropping mercury electrode was used, 1 M sodium sulphate, 0.4 M sodium chloride and 0.5 M boric acid were used as the base solution. A cell of volume 100 cm^3 was employed. The temperature was maintained constant at 25 ± 1° C. All potentials were referred to a saturated calomel electrode (SCE).

2.2. *Chemicals and electrode materials*

Nickel sulphate ($NiSO_4$), nickel chloride ($NiCl_2$) and boric acid (H_3BO_3) were guaranteed reagents of Wako Pure Chemical Industries, Ltd. Saccharin ($C_7H_4NO_3S{\cdot}Na$) and three kinds of aliphatic alcohols (*n*-propyl alcohol ($CH_3CH_2CH_2OH$), allyl alcohol ($CH_2{=}CHCH_2OH$) and propargyl alcohol ($CH{\equiv}CCH_2OH$)) were guaranteed reagents of Tokyo Kasei Kogyo Co., Ltd. All chemicals were used without further purification. Solutions were prepared in redistilled water.

Low carbon steel plate (Nishin Steel Co.) of 10 cm^2 surface area was used as the cathode. The precleaning procedure was as follows [8, 9]. Low carbon steel plate was degreased in alkaline solution (Dipsol Chemical Co., Ltd, No. 44-S, 40 g dm^{-3}) at about 50–60° C for 30 min. It was then electropolished in alkaline solution (Dispol Chemical Co., Ltd. NC-10, 100 g dm^{-3}) at 10 A dm^{-2} for 1 min. A nickel metal plate (Yoneyama Chemical Industries, Ltd, 99.9%) of approximate 10 cm^2 surface area was used as the anode.

3. Results and discussion

3.1. *Adsorption of organic additives on the dropping mercury electrode*

Electrocapillary curves for saccharin and three kinds of aliphatic alcohols in the base solution (1 M Na_2SO_4 + 0.4 M NaCl + 0.5 M H_3BO_3) are shown in Fig. 1. When saccharin, *n*-propyl alcohol, allyl alcohol or propargyl alcohol were added, decreases in the drop time of mercury from the curve of the base solution were observed. These decreases in the drop time imply that saccharin and the aliphatic alcohols are adsorbed on the dropping mercury electrode. In the electrocapillary curve for saccharin (Fig. 1, curve b), the drop time of mercury decreased in the potential range 0 to −1.2 V. When *n*-propyl alcohol, allyl alcohol or propargyl alcohol were added (Fig. 1, curves c–e), decreases in the drop time were observed in the range 0 to −1.3 V. The differences in the mercury drop time between the base solution and the solution containing aliphatic alcohol became progressively larger in the order *n*-propyl alcohol, allyl alcohol and propargyl alcohol (that is, with increasing degree of unsaturated linkage in the aliphatic alcohol molecule, namely in the order C–C, C=C and C≡C). The above results suggest that the adsorbability on the electrode increases in the order *n*-propyl alcohol, allyl alcohol and propargyl alcohol.

3.2. *Current–potential curves under potentiostatic conditions*

Figure 2 shows current–potential curves for the Watts bath (1 M $NiSO_4$ + 0.2 M $NiCl_2$ + 0.5 M H_3BO_3) in the absence or presence of organic additives using low carbon steel as the cathode under potentiostatic conditions. These curves were obtained by plotting the

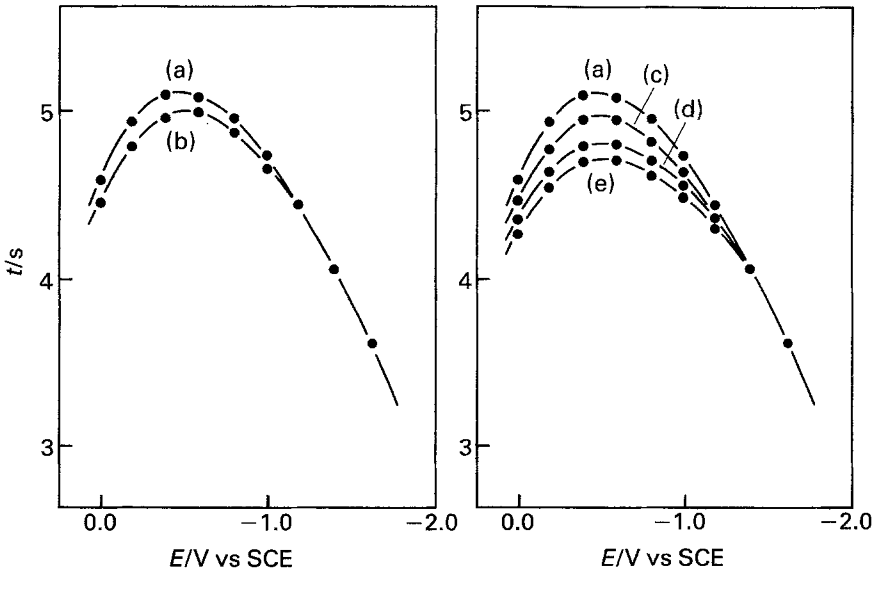

Fig. 1. Electrocapillary curves of saccharin and aliphatic alcohols: (a) 1 M Na_2SO_4 + 0.4 M NaCl + 0.5 M H_3BO_3; (b) (*a*) + 10 mM saccharin; (c) (*a*) + 10 mM *n*-propyl alcohol; (d) (*a*) + 10 mM allyl alcohol; (e) (*a*) + 10 mM propargyl alcohol.

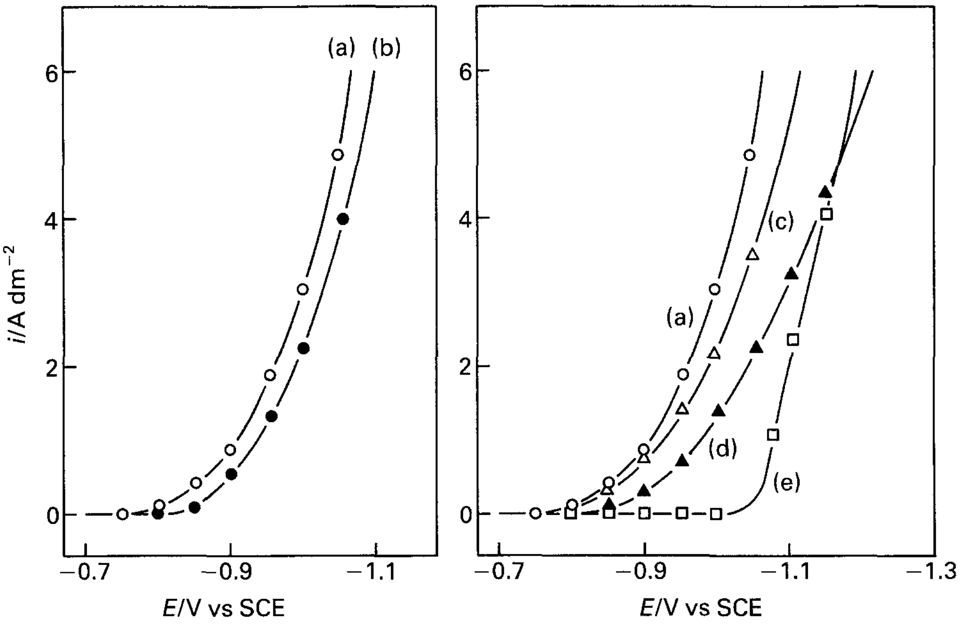

Fig. 2. Current–potential curves of nickel ion in the presence of saccharin or aliphatic alcohols under potentiostatic conditions: (a) 1 M $NiSO_4$ + 0.2 M $NiCl_2$ + 0.5 M H_3BO_3; (b) (*a*) + 5 mM saccharin; (c) (*a*) + 5 mM *n*-propyl alcohol; (d) (*a*) + 5 mM allyl alcohol; (e) (*a*) + 5 mM propargyl alcohol.

steady state current against the applied potential. In the absence of organic additives the current increased gradually from the negative potential of −0.75 V due to the reduction of nickel ion (Ni^{2+}) (Fig. 2, curve a). When saccharin was added, the reduction potential of nickel ion shifted to a more negative potential by about 0.1 V (Fig. 2, curve b) because of the inhibitory effect of saccharin on the reduction of nickel ion. As for the current–potential curves in the presence of *n*-propyl alcohol or allyl alcohol (Fig. 2, curves c and d), the reduction potentials of nickel ion were shifted to more negative potentials, and at the same time the slope of the ascending portion of the current became smaller in the order *n*-propyl alcohol and allyl alcohol. On the other hand, when propargyl alcohol was added (Fig. 2, curve e), the nickel ion reduction current was strongly inhibited in the range −0.75 to −1.00 V and the current increased abruptly at the negative potential of −1.00 V. It can be concluded that the inhibitory effects of aliphatic alcohols on the reduction of nickel ion become stronger in the order *n*-propyl alcohol, allyl alcohol and propargyl alcohol (that is, with increasing adsorbability of the aliphatic alcohol).

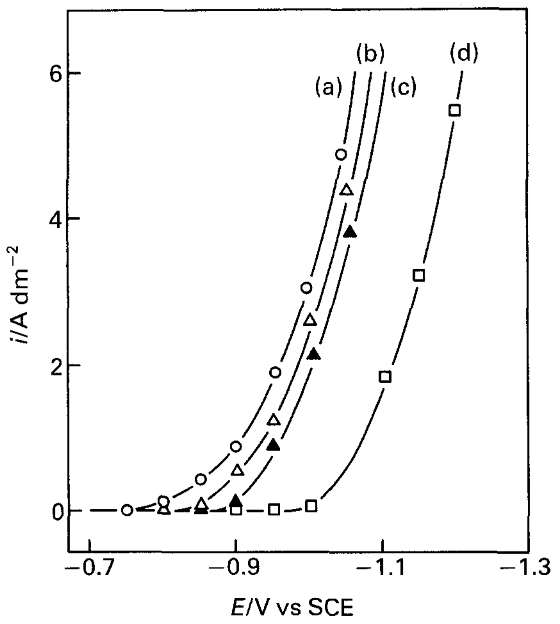

Fig. 3. Current–potential curves of nickel ion in the presence of saccharin and aliphatic alcohols under potentiostatic conditions: (a) 1 M $NiSO_4$ + 0.2 M $NiCl_2$ + 0.5 M H_3BO_3; (b) (*a*) + 5 mM saccharin + 5 mM *n*-propyl alcohol; (c) (*a*) + 5 mM saccharin + 5 mM allyl alcohol; (d) (*a*) + 5 mM saccharin + 5 mM propargyl alcohol.

Figure 3 shows current–potential curves for the Watts bath in the presence of both saccharin and aliphatic alcohols. It can be seen from Fig. 3, curves b–d that the deposition potentials of nickel were shifted towards negative potentials in the presence of aliphatic alcohols. The potential range in which the nickel ion reduction was inhibited became greater in the order *n*-propyl alcohol, allyl alcohol and propargyl alcohol. These results imply that in the presence of both saccharin and aliphatic alcohols, the inhibitory effect on the reduction of nickel ion also becomes stronger in the order *n*-propyl alcohol, allyl alcohol and propargyl alcohol.

3.3. *Surface morphology of electrodeposited nickel*

Scanning electron micrographs (SEM) of electrodeposited nickel from the Watts bath in the absence or presence of saccharin under galvanostatic condition (5.0 A dm^{-2}), are shown in Fig. 4. It can be seen that in the absence of organic additives (Fig. 4(a)) large granular crystals (2–5 μm) were observed on the whole surface and the surface roughness was relatively large. Consequently, it became apparent

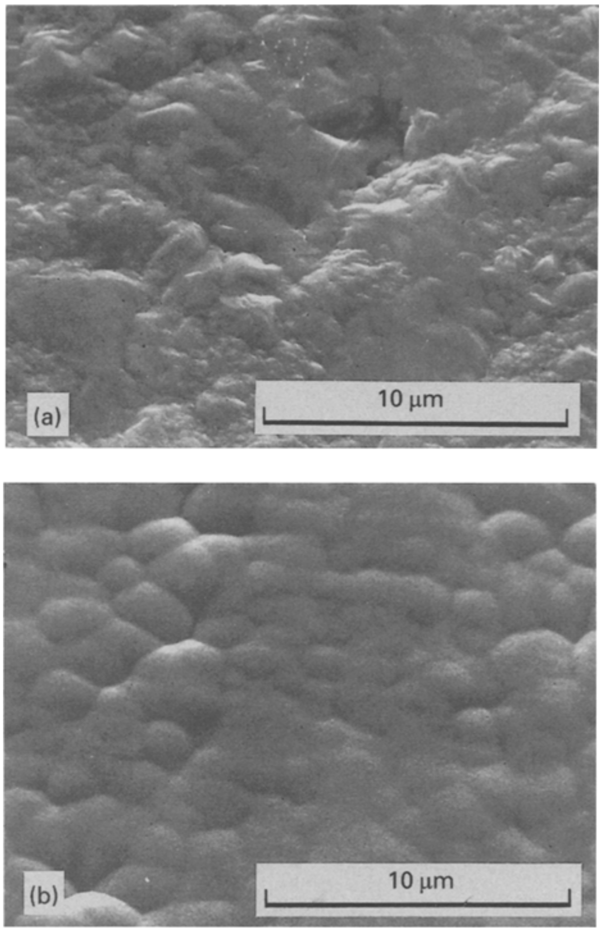

Fig. 4. Scanning electron micrographs of electrodeposited nickel in the absence or presence of saccharin ($5.0\,\mathrm{A\,dm^{-2}}$, 5 min): (a) 1 M $NiSO_4$ + 0.2 M $NiCl_2$ + 0.5 M H_3BO_3; (b) (*a*) + 5 mM saccharin.

that smooth and fine-grained nickel electrodeposits cannot be obtained when organic additives are not present. On the other hand, when saccharin was added, the size of granular aggregated crystals became smaller and the surface roughness was relatively small (Fig. 4(b)). This may be ascribed to the inhibitory effect of saccharin on the nickel ion reduction.

Figure 5 shows SEMs for a Watts bath containing *n*-propyl alcohol, allyl alcohol or propargyl alcohol alone under galvanostatic condition ($5.0\,\mathrm{A\,dm^{-2}}$). When *n*-propyl alcohol or allyl alcohol were added (Fig. 5(a) and (b)), the surface morphology was analogous to that obtained in the absence of the organic additives (Fig. 4(a)). That is, block-like or granular crystals were observed. It can be seen from Fig. 5 that the size of aggregated crystals became smaller in the order *n*-propyl alcohol, allyl alcohol and propargyl alcohol. Especially, propargyl alcohol gave fine-grained electrodeposits of nickel (Fig. 5(c)). Thus propargyl alcohol, which has the strongest inhibitory effect on the reduction of nickel ion among the three kinds of aliphatic alcohols (Fig. 2, curve e), has a grain refinement action. However, when propargyl alcohol was added alone, no nickel deposited parts were also observed with SEM of low magnifications, which will be shown later.

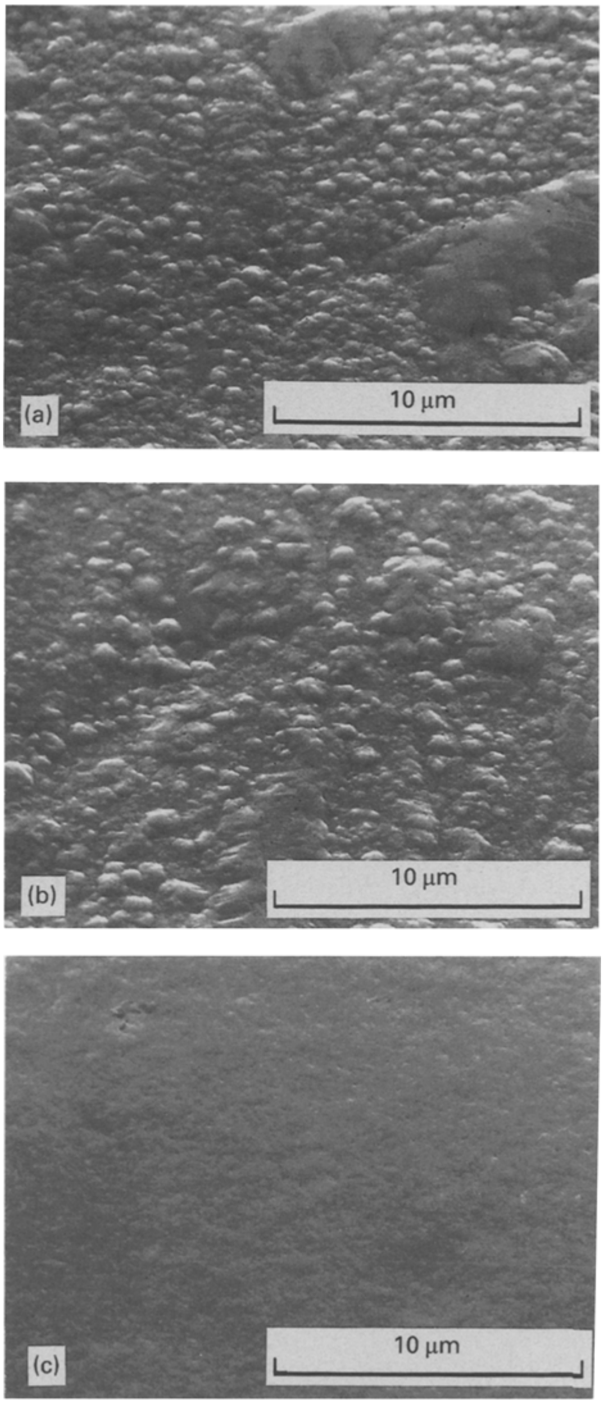

Fig. 5. Scanning electron micrographs of electrodeposited nickel in the presence of aliphatic alcohols ($5.0\,\mathrm{A\,dm^{-2}}$, 5 min): (X) 1 M $NiSO_4$ + 0.2 M $NiCl_2$ + 0.5 M H_3BO_3; (a) (X) + 5 mM *n*-propyl alcohol; (b) (X) + 5 mM allyl alcohol; (c) (X) + 5 mM propargyl alcohol.

Figure 6 shows the SEM and the corresponding X-ray elemental map ($\mathrm{Fe}K_{\alpha}$) of electrodeposited nickel obtained in the presence of propargyl alcohol alone at a current density of $3.0\,\mathrm{A\,dm^{-2}}$. By means of SEM observation with low magnifications (1/50th of those for Fig. 5(c)), the exposed parts of the surface of the steel used as the substrate were seen to be large (Fig. 6(b)). It became apparent from Fig. 6 that nickel did not deposit uniformly on the surface in the presence of propargyl alcohol alone. Similar results were obtained at $5.0\,\mathrm{A\,dm^{-2}}$, but the area of the exposed parts was small.

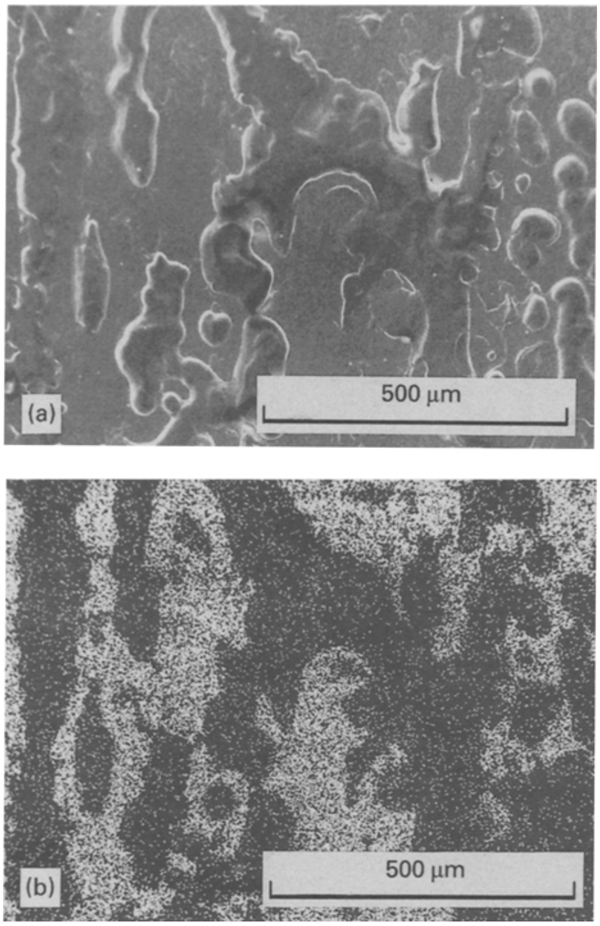

Fig. 6. Scanning electron micrograph and X-ray elemental map of electrodeposited nickel in the presence of propargyl alcohol: (a) Scanning electron micrograph (1 M $NiSO_4$ + 0.2 M $NiCl_2$ + 0.5 M H_3BO_3 + 5 mM propargyl alcohol, 3.0 A dm^{-2}, 5 min); (b) X-ray elemental map (FeK_{α}) of corresponding (a).

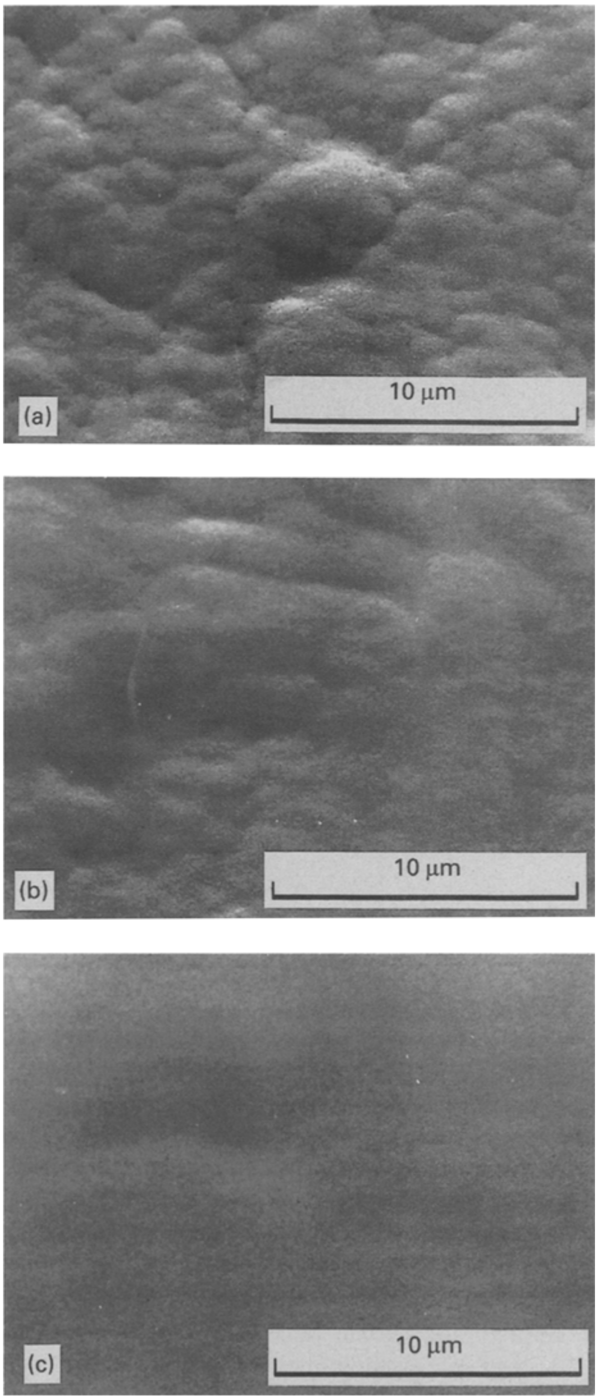

Fig. 7. Scanning electron micrographs of electrodeposited nickel in the presence of saccharin and aliphatic alcohols (5.0 A dm^{-2}, 5 min): (X) 1 M $NiSO_4$ + 0.2 M $NiCl_2$ + 0.5 M H_3BO_3 + 5 mM saccharin; (a) (X) + 5 mM *n*-propyl alcohol; (b) (X) + 5 mM allyl alcohol; (c) (X) + 5 mM propargyl alcohol.

Figure 7 shows the SEM obtained in the presence of both saccharin and aliphatic alcohols at 5.0 A dm^{-2}. When saccharin and aliphatic alcohols were added, fine-grained and compact electrodeposits were obtained due to the synergistic effect of the two kinds of adsorbed species [7, 10, 11]. Also in these cases, the size of aggregated crystals and surface roughness became smaller in the order *n*-propyl alcohol, allyl alcohol and propargyl alcohol. As described above, the adsorbability and the inhibitory effects on the nickel ion reduction increased in the same order (Fig. 1, curves c–e, Fig. 2, curves c–e). Further, the deposition potentials at 5.0 A dm^{-2} in the presence of both saccharin and aliphatic alcohols were shifted to more negative values in the order *n*-propyl alcohol, allyl alcohol and propargyl alcohol (Fig. 3, curves b–d). Consequently, the nucleation dependent growth of nickel may occur preferentially, and the crystal grain size may, therefore, be smaller [7, 12, 13]. In the case where saccharin and propargyl alcohol are present, the shift of the deposition potential was large due to the strong inhibitory effect of conjugated saccharin and propargyl alcohol on the reduction of the nickel ion (Fig. 3, curve d). Therefore, fine-grained, smooth and compact electrodeposits of nickel are obtained by adding both saccharin and propargyl alcohol (Fig. 7(c)).

Similar results were obtained in the range of current densities 1.0 to 3.0 A dm^{-2}.

3.4. *Crystal orientation of electrodeposited nickel*

X-ray diffraction patterns of electrodeposited nickel, in the absence or presence of saccharin, *n*-propyl alcohol, allyl alcohol or propargyl alcohol alone under galvanostatic condition (5.0 A dm^{-2}), are shown in

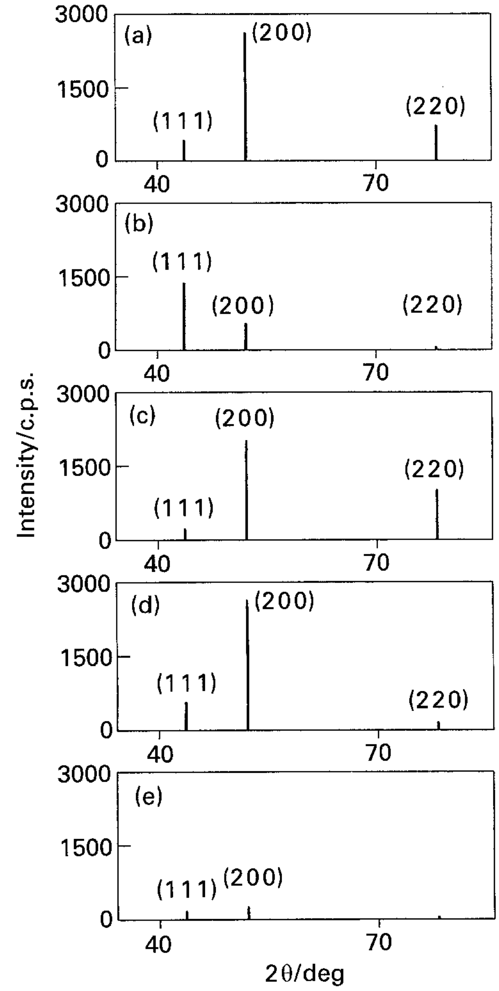

Fig. 8. X-ray diffraction patterns of electrodeposited nickel in the presence of saccharin or aliphatic alcohols (5.0 A dm^{-2}, 5 min): (a) 1 M $NiSO_4$ + 0.2 M $NiCl_2$ + 0.5 M H_3BO_3; (b) (*a*) + 5 mM saccharin; (c) (*a*) + 5 mM *n*-propyl alcohol; (d) (*a*) + 5 mM allyl alcohol; (e) (*a*) + 5 mM propargyl alcohol.

Fig. 8. Electrodeposited nickel obtained in the absence of organic additives exhibited a (2 0 0) diffraction peak of strong intensity and (1 1 1) and (2 2 0) peaks with relatively weak intensities (Fig. 8(a)). This suggests a preferred orientation with the (2 0 0) plane parallel to the surface. When saccharin was added, the (1 1 1) peak increased in intensity while the (2 0 0) and (2 2 0) peaks weakened (Fig. 8(b)). On the other hand, when *n*-propyl alcohol or allyl alcohol were added alone, X-ray diffraction patterns were analogous to those obtained in the absence of organic additives, in which a (2 0 0) peak of strong intensity was observed (Fig. 8(c) and (d)). However, the electrodeposit obtained in the presence of propargyl alcohol exhibited (1 1 1) and (2 0 0) peaks of weak intensity (Fig. 8(e)) because a uniform deposition of nickel over the whole surface was not obtained in this case (Fig. 6).

Figure 9 shows X-ray diffraction patterns of electrodeposited nickel obtained in the presence of both saccharin and aliphatic alcohols at 5.0 A dm^{-2}. In these cases, a (1 1 1) peak of strong intensity was observed (Fig. 9(a)–(c)) and the diffraction patterns were similar to those of electrodeposits obtained by adding saccharin alone (Fig. 8(b)). Thus the effect of saccharin may appear stronger than those of aliphatic alcohols on the crystal orientation of electrodeposited nickel. Consequently, when saccharin and aliphatic alcohols were added, nickel with a preferred orientation with the (1 1 1) plane parallel to the surface was obtained.

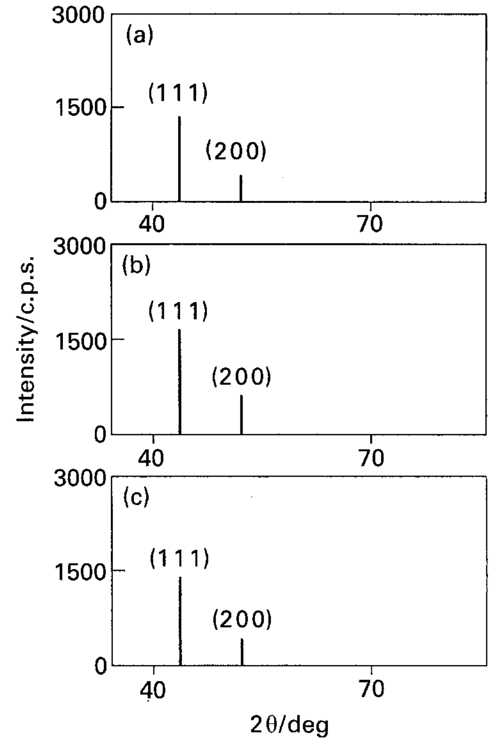

Fig. 9. X-ray diffraction patterns of electrodeposited nickel in the presence of saccharin and aliphatic alcohols (5.0 A dm^{-2}, 5 min): (X) 1 M $NiSO_4$ + 0.2 M $NiCl_2$ + 0.5 M H_3BO_3 + 5 mM saccharin; (a) (X) + 5 mM *n*-propyl alcohol; (b) (X) + 5 mM allyl alcohol; (c) (X) + 5 mM propargyl alcohol.

References

[1] H. Brown and B. B. Knapp, *in* 'Modern Electroplating', 3rd edn (edited by F. A. Lowenheim), John Wiley & Sons, New York (1974) p. 287.

[2] J. K. Dennis and T. E. Such, *in* 'Nickel and Chromium Plating', Newnes–Butterworths, London (1972) p. 92.

[3] R. Weil and W. N. Jacobus Jr., *Plating* **53** (1966) 102.

[4] I. Epelboin, M. Froment and G. Maurin, *Plating* **56** (1969) 1356.

[5] Th. Ap. Costavaras, M. Froment and A. Hugot-Le Goff, *J. Electrochem. Soc.* **120** (1973) 867.

[6] St. Rashkov and N. Atanasov, *Electrodep. Surf. Treat.* **3** (1975) 105.

[7] N. Kaneko, N. Shinohara, Y. Itoh and H. Nezu, *Bunseki Kagaku* **40** (1991) 655.

[8] H. Nezu, N. Kaneko and N. Shinohara, *Kinzoku Hyomen Gijutsu* **31** (1980) 244.

[9] N. Kaneko, N. Shinohara and H. Nezu, *Electrochim. Acta*, in press.

[10] O. Kardos and D. G. Foulke, *in* 'Advances in Electrochemistry and Electrochemical Engineering', Vol 2 (edited by C. W. Tobias), Interscience Publishers, New York (1962) p. 145.

[11] K. Boto, *Electrodep. Surf. Treat.* **3** (1975) 77.

[12] N. Kaneko and H. Nezu, *J. Appl. Electrochem.* **19** (1989) 387.

[13] N. Kaneko, N. Shinohara and H. Nezu, *Electrochim. Acta* **36** (1991) 985.